The International Journal of Engineering and Science (IJES)
|| Volume || 13 || Issue || 8 || Pages || PP 79-92 || 2024 ||
ISSN (e): 2319 – 1813 ISSN (p): 2319 – 1805

# Unsteady Magnetohydrodynamic Flow of A Dusty Williamson Nanofluid over a Stretching Cylinder in a porous medium with effect of Hartman number and volume fractions

Adekanmbi- Akinseye Adejoke [1], Fenuga Olugbenga[2] , Aroloye Joseph[2]
Email:upvictory@yahoo.co.uk
[1] *Department of Mathematics, faculty of science, University of Lagos, Nigeria*
[2]: *Department of Mathematics, University of Lagos, Nigeria*

----------***ABSTRACT***----------
*This work focuses on investigating the characteristics of an unsteady Williamson Magneto hydrodynamic (MHD) boundary layer nanofluid flow past a Stretching Cylinder that is permeable and in a porous medium. The modeled partial differential equation is transformed into coupled non linear ordinary differential equation for both fluid and dust phases through a similarity variable transformation and the resulting systems are solved analytically using the Homotopy Perturbation Method (HPM). The comparison of the HPM results with the numerical scheme of the fourth order Runge Kutta integration with shooting technique are in excellent agreement by using some published literature. The current study examines the impact of the Hartman number and volume fractions of the dusty particle on the velocity, temperature and concentration profiles for the two phases and are graphically presented while the influence of pertinent parameter of physical engineering interest on the skin friction coefficient, Nusselt number and Sherwood number are presented through tables. The present result has been compared with some published works in literature and are found to be in excellent agreement. The results shows that Increasing the volume fraction of the dust particles enhance the heat transfer rate of both phases and reduces the friction factor. Also increasing values of Hartman number decreases the velocity profile as well as the momentum boundary layer thickness and increases temperature profile of the fluid and the dust phases.*

***KEYWORDS;*** *Hartman number, volume fraction, Dusty particles, unsteady flow , stretching cylinder*

---

Date of Submission: 24-08-2024 Date of acceptance: 03-09-2024

---

## I. INTRODUCTION

Based on their fluid flow properties, fluids are typically categorized into two separate groups: Newtonian and non-Newtonian fluids. . Newtonian fluids, which derive their name from Sir Isaac Newton, exhibit a linear relationship between their rate of deformation and the shear stress, therefore adhering to Newton's law of viscosity. The rate of deformation does not have an impact on the viscosity. In recent times, there has been significant progress in the field of non-Newtonian fluid investigations. The Williamson model is a specific non-Newtonian model that was developed to accurately represent the flow behavior of pseudo plastic materials. Williamson[1], explored the rheological behavior of pseudo plastic materials that behaves like plastic but are not plastic. He found that, a good model to describe the movement of pseudoplastic fluids is the Williamson equation and subsequently conducted experiments to validate the obtained results. Subbarayudu et al. [2] analysed the assessment of the time-varying movement of a Williamson fluid with radioactive movement of blood in the presence of a wedge. Hashim et al. [3] performed an investigation on the transient flow of Williamson nanofluids with convective heat transfer using magnetohydrodynamics (MHD), examining different solutions. Fluid flow in porous media is extensively employed in various fields such as material processing, thermal energy transfer, oil exploration, fuel cell technology, and flow bed chromatography. A highly effective method for enhancing thermal efficiency is the combined effect of heat transfer and variations in temperature across the boundary layer of nanofluid flows through a porous media in the presence of an external magnetic field. A number of research scholars have been investigating the movement and behaviour of fluids within porous materials with a particular emphasis on different challenges. Jiang and Ren [4] conducted a study on forced con-vection in a porous material utilizing a thermal unsteady model. A major goal of thermal engineering

is to enhance the thermal characteristics of heat transfer fluids. By introducing nanosized solid particles (ranging from 1 to 100 nm) into the fluid, can enhance the base fluid's heat transfer properties and thermal conductivity. Usually, these nanoparticles are composed of metals, carbon nanotubes, oxides, or carbides. The augmentation of heat transmission in fluids due to the dispersion of extremely small particles was initially documented by Masuda et al. [5]. Choi and Eastman [6] coined the term 'nanofluid' to describe a fluid that contains dispersed nanoparticles. Extensive research on the interaction between a magnetic field and an electrically conducting fluid was investigated by Elboughdiri et al. [7]. Magneto hydrodynamics (MHD) is the study of how a magnetic field interacts with an electrically conducting fluid. It combines the principles of fluid mechanics with electromagnetism to describe this behavior. Alfven was the first to begin exploring this topic in 1942, [8]. He introduced MHD water-based nanofluids with convective boundary conditions Alfvén [8].

Magneto hydrodynamics is utilized in several fields such as tissue temperature regulation, blood flow analysis, cell separation techniques, endoscope procedures, and cancer tumor therapy, Amjad et. al [9]. The MHD Williamson nanofluid is gaining increasing attention for research. Reddy et al. [10] examined the properties of heat transport and Williamson MHD Nanofluid flow as it passes across a porous plate. The study of magneto MHD flow properties has gained popularity due to the impact of magnetic fields on the performance and flow management of different systems involving electrically conducting fluids, such as liquid metals and water with a little acid content. The term nanofluid refers to a homogeneous mixture of nanoscale solid particles such as oxides, silica, polymers, metals, non metals, and carbon nanotubes with common fluids such as water, oils and alcohols. The primary goal of nanofluid development is to achieve the highest thermal conductivity with a low concentration of nanoparticles through the uniform distribution and suspension of nanoparticles in base fluids. Abbas[11]. Noble technology has been created to enhance thermal conductivity of heat transfer fluids to achieve energy saving and environmental cleaning. This method involves combining nanoparticles with a base liquid. Nanoparticles have important thermo physical properties compared to traditional fluids, which improves the conductivity of heat of traditional fluid. Researchers have employed various strategies and techniques can be to enhance the efficiency of fluids. These fluids are often referred to as "nanofluids" and are made by breaking up small particles of less than 100 nm in size into ordinary fluids. Mahdi et al. [12] performed an investigation on the movement of nanofluid and the transmission of heat by convection in porous materials. The study of the fluid dynamics of a stretched cylinder and its various properties has become a highly sought-after field of research in recent years. This phenomenon has practical requirements in a variety of industrial and technical operations, such as polymer extrusion, creation of synthetic fibers, paper production, water supply systems, copper wire production, metal extrusion and others. Kothandapani and Srinivas [13] conducted a research on the phenomenon of peristaltic MHD transport and heat transfer in a porous medium with the presence of walls. Although few authors have studied Williamson and nanofluid separately, over stretching cylinder and plate with a number of publications up to some extent. To the best of the author's knowledge, there has been sparse research work in the literature that considers heat and mass transfer of a dusty Williamson MHD nanofluid flow over a permeable stretching cylinder in a porous medium. Also researchers realized the difficulty of nonlinear coupled equations and have not been able to solve this problem using analytical method. Therefore this is the first time analytical solution is established for the problem, Adekanmbi-Akinseye et al. [14]. Motivated by the above limitations and the gaps in the past research works, an attempt is made in this study to examine theoretically the problem of boundary layer flows, heat and mass transfer of viscous, incompressible, electrically conducting, dusty Williamson MHD nanofluid flow over a permeable horizontally placed stretching cylinder in a porous medium.

## II. MATERIALS AND METHODS

Figure 1 depicts the schematic diagram illustrating the two-dimensional dusty Williamson MHD nanofluid on a stretching cylinder through a porous medium. Temperature, velocity and concentration on the surface are denoted by$T_w$, $U_w$ and C respectively whilst the ambient fluid temperature, velocity and concentration are denoted by $T_\infty$ ,$U_\infty$ and $C_\infty$respectively. Furthermore, w and u are the velocity components in the direction of z and r axis respectively.

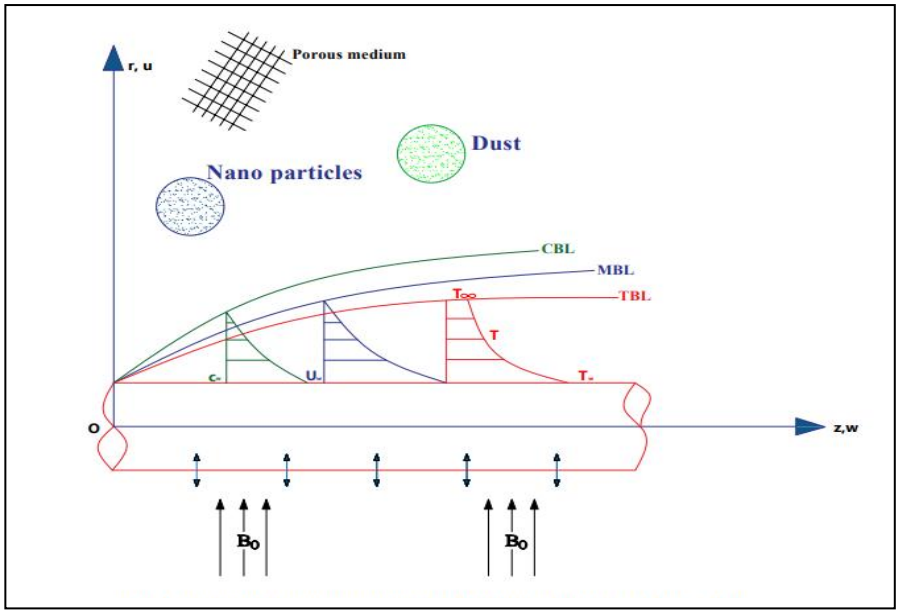


The following assumptions are made:

I. The r-axis is orthogonal to the z-axis, which is aligned with the axis of the cylinder.
II. The circular surface experiences thermal gradient.
III. Due to the modest value of the magnetic Reynolds number, the in-duced magnetic field is significantly smaller than the applied mag-netic field.
IV. The impact of the collision between nanoparticles and dust is insigni-ficant.
V. The viscosity coefficient and thermal conductivity of the thermal flu-id vary, but the permeability coefficient of the porous media remains constant.
VI. Both the fluid and porous media are in a state of constant temperature equilibrium and there is no slippage between them.

The governing boundary layer equations under each of the aforementioned assumptions are as follows

2.1 **Equations of the heat and mass governing the problem:**

**2.1.1 FOR THE** WILLIAMSON FLUID **PHASE**

**Continuity equation**

$$\frac{\partial(ru)}{\partial r}+\frac{\partial(rw)}{\partial z}=0 \tag{1}$$

**The momentum equation:**

$$u\frac{\partial w}{\partial r}+w\frac{\partial w}{\partial z}=\upsilon_{nf}\left(\frac{1}{r}\frac{\partial W}{\partial r}+\frac{\partial^2 \mathrm{W}}{\partial \mathrm{r}^2}\right)+\upsilon_{nf}\left[\frac{\Gamma}{\sqrt{2}}\left(\frac{\partial T}{\partial r}\right)^2+\sqrt{2}\frac{\partial w}{\partial r}\frac{\partial^2}{\partial r^2}\right]+\frac{\mathrm{KN}}{\rho_{\mathrm{nf}}}\left(\mathrm{w_p}-\mathrm{w}\right)-\left(\frac{\sigma \mathrm{B}_0^2}{\rho_{\mathrm{nf}}}+\frac{\upsilon_{\mathrm{nf}}}{\mathrm{k_p}}\right)\mathrm{w} \tag{2}$$

**The Energy equation**

$$w\frac{\partial T}{\partial z}+u\frac{\partial T}{\partial r}=\frac{k}{\rho \mathrm{c_P}}\left(\frac{1}{r}\frac{\partial T}{\partial r}+\frac{\partial^2 \mathrm{T}}{\partial \mathrm{r}^2}\right)+\tau\left\{D_B\frac{\partial C}{\partial r}\frac{\partial T}{\partial r}+\frac{D_T}{T_\infty}\left(\frac{\partial T}{\partial r}\right)^2\right\}+\frac{\mathrm{Q_0}}{(\rho \mathrm{c_P})}(\mathrm{T}-\mathrm{T}_\infty) \tag{3}$$

**The Concentration equation**

$$w\frac{\partial C}{\partial z}+u\frac{\partial C}{\partial r}=D_B\frac{\partial^2 \mathrm{C}}{\partial \mathrm{r}^2}+\frac{D_T}{T_\infty}\left(\frac{\partial^2 \mathrm{T}}{\partial \mathrm{r}^2}\right) \tag{4}$$

### 2.1.2 FOR THE DUST PHASE

**Continuity equation** (5)

$$\frac{\partial(ru_p)}{\partial r}+\frac{\partial(rw_p)}{\partial z}=0,$$

**Momentum equation**

$$w_p\frac{\partial w_p}{\partial r}+u_p\frac{\partial w_p}{\partial z}=\frac{K}{\rho}(w-w_p) \quad (6)$$

**Energy equation**

$$w_p\frac{\partial T_p}{\partial r}+u_p\frac{\partial T_p}{\partial z}=\frac{Cp_f}{T_tCp}(T-T_p) \quad (7)$$

**Concentration equation**

$$w_p\frac{\partial C_p}{\partial r}+u_p\frac{\partial C_p}{\partial z}=\frac{mN}{\rho T_c}(C-C_p) \quad (8)$$

Equations (1)–(4) are for the fluid phase and Equations (5)–(8) are for the dust phase

where (w, u) and $(w_p u_p)$ are the velocity components of the nanofluid and dust phases, in the z and r directions respectively. ν, ρ, N, m, K, $and\ k_0$ are the kinematic viscosity of the fluid, density of the fluid, number density of the particle phase, mass of the dust particle, Stoke's resistance (drag co-efficient) and permeability of the porous medium respectively, in addition, α represent the thermal diff usivity, ρ refer to density of the fluid. The associated boundary conditions are as follows

Fluid:

$$\left.\begin{array}{l} w=U_w,\ u=0, \mathrm{T}=T_w=T_\infty, \mathrm{C}=C_w=C_\infty \quad \text{at r = a} \\ w\to 0\ \ u=0, \mathrm{T}\longrightarrow T_\infty \quad T_P \quad T_\infty \longrightarrow \mathrm{C} \quad C_\infty \longrightarrow \text{as r} \quad \infty \longrightarrow \end{array}\right\} \quad (9)$$

Dust:

$$\left.\begin{array}{l} w_P=U_w,\ u_p=0, \mathrm{T_p}=T_w=T_\infty, \mathrm{C_p}=C_w=C_\infty \quad \text{at r = a} \\ w\to 0\ w_P\longrightarrow 0,\ u_p\longrightarrow u, \mathrm{T_p}\longrightarrow T_\infty, , \mathrm{C}\longrightarrow C_\infty \mathrm{C_p}\longrightarrow C_\infty \quad \text{as r} =\infty \end{array}\right\} \quad (10)$$

In order to transform the governing equations into the appropriate ordinary differential equations (ODEs), the following similarity variables are introduced.

$$\eta=\frac{r^2-a^2}{2a}\sqrt{\frac{u_W}{\nu z}},\ \psi=a\sqrt{\nu_f u_w z}\,\mathrm{f}(\eta),\ \theta=\frac{T-T_\infty}{T_w-T_\infty},\ w=u_w(z)f'(\eta),\ u=-\frac{a}{r}\sqrt{\frac{\nu_f u_w}{z}}f(\eta), \quad (11)$$

And dust phase:

$$\psi_P=\sqrt[a]{\nu_f u_w z}F(\eta),\ u_p=-\frac{a}{r}\sqrt{\frac{\nu_f u_w}{z}}F(\eta), w_p=u_w(z)F'(\eta),\quad \theta_p(\eta)=\frac{T_p-T_\infty}{T_w-T_\infty} \quad (12)$$

The stream function, $\psi$, that satisfies the continuity equation is presentedwith the velocity components$u=-\frac{1}{r}\frac{\partial\psi}{\partial r}$ $and\ w=-\frac{1}{r}\frac{\partial\psi}{\partial z}$. The variables η, f, and θ represent the dimensionless transverse distance, dimensionless stream function, and dimensionless temperature of the fluid, respectively. The kinematic viscosity $\nu=\frac{\mu_\infty}{\rho}$.. After applying above transformations to the governing equations we obtain the following dimensionless form of the three equations

**Fluid phase**

$$\phi_1\left\{(1+2\gamma\eta)f'''+2\gamma f''\right\}+\phi_1 We(1+2\gamma\eta)^{\frac{1}{2}}\left[\gamma f''^2+2\left\{\gamma f''+(1+2\gamma\eta)f'''\right\}\right]$$
$$+\phi_2\left(ff''-f'^2\right)-\beta\beta_v\left(f'-F'\right)-\left(\phi_5 Ha+\phi_1 Da\right)f'=0 \quad (13)$$

$$\frac{\phi_1\phi_4}{Pr}\left\{(1+2\gamma\eta)\theta''+2\gamma\theta'\right\}+\phi_1\phi_3\left(\theta' f-2\theta f'\right)$$
$$+\phi_1\phi_2 Ha\cdot Ec\left(f'\right)^2+\frac{\phi_2\phi_4}{Pr}\left(Af'+B\theta\right)+\phi_1\beta_T\beta\left(\theta_p-\theta\right)=0 \quad (14)$$

$$\phi''+Scf\boldsymbol{\phi}'+\left(\frac{\mathbf{N_T}}{\mathbf{N_B}}\right)\theta''+\beta_c\left(\phi_p-\phi\right)=0 \quad (15)$$

**Dust phase**

$$F'^2-FF''-\beta_v\left(f'-F'\right)=0 \quad (16)$$

$$\theta_p'F-2\theta_pF'+\gamma^*\beta_T\left(\theta-\theta_p\right)=0 \quad (17)$$

$$\phi_p'F-2\phi_pF'+l\beta_cH\left(\phi_p-\phi\right)=0 \quad (18)$$

**And the corresponding Dimensionless BCs are listed below**

$$\left.\begin{aligned} &f(\eta)=0, f'(\eta)=1,\ \theta(\eta)=0 \quad \phi=0 \quad at\ \eta=0,\\ &f(\eta)=0,\ F'(\eta)=0, F(\eta)=f(\eta)\theta(\eta)=0, \theta_p(\eta)=0, \phi=0, \phi_p=0 \quad as\ \eta=\infty \end{aligned}\right\} \quad (19)$$

The dimensionless equations contain the following emergent parameters:

$\mathrm{P_r}=\frac{\mu c_p}{k}$, is Prandtl number. $Ha=\frac{\sigma_f B_0 w}{\rho_f U_f}$ is Hartman number,

$\gamma=\frac{1}{a}\sqrt{\frac{\nu_f z}{u_w}}$ is Curvature parameter, $K=\frac{z}{\tau u_w}$, is porosity parameter, $Ec=\frac{u_w z}{Ac_p}$ is Eckert,,

$\beta=h_0\left(\frac{2v}{U_\infty}\right)^{-1/2}$ is thefluid particle interaction, $S=\frac{vz}{k_p u_w}$ is the permeability Parameter

$\lambda=\Gamma\sqrt{\frac{2u_w}{v_{nf}z}}$ is the Weissenberg parameter, $R_e=\frac{{U_w}^3(z)}{vL}$ is the Reynold's number,

$Q=\frac{\sigma B_0^2}{\rho_{nf}u_w}$ is first order heat source/sink, $Da=\frac{u_w}{k_p\rho_f z}$ is Darcy

$N_t=\frac{\tau D_T}{vT_\infty}(T_w-T_\infty)$ is the thermophoresis parameter, $N_b=\frac{\tau D_B}{v}(C_w-C_\infty)Brownian$ motion, (20)

$l=\frac{mN}{\rho_p}\longrightarrow$ mass concentration $Sc=\frac{\nu}{D_B}\longrightarrow$ Schimdt number

2 2 .**Parameters of physical and engineering interest for the problem**

The engineering-related physical quantities of importance are skin friction coefficient, $(C_f)$, Nusselt number (Nu) and Sherwood number (Sh) which, in turn, physically represent the wall shear stress, heat transfer rate and

mass transfer rate respectively They each have the following definitions: Skin friction coefficient,Nusselt numberand Sherwood number defined as

$$C_{fz} = \frac{\tau_w}{\rho_{nf} U_w} \ ,$$

$$Nu_z = \frac{q_w}{k_f(T_w - T_\infty)}$$

$$S\square_z = \frac{m_w}{Dm_\infty (C_w - C_\infty)} \qquad (21)$$

$\tau_w$Is the shearing stress, $q_w$ is the heat flux and $m_w$is the mass flux at the surface and $Dm_\infty$is the diffusion constant respectively and defined as

$$\tau_w = \mu_{nf}\left[\frac{\partial u}{\partial r} + \frac{\Gamma}{\sqrt{2}}\left(\frac{\partial u}{\partial r}\right)^2\right]_{r=a}$$

$$q_w = -k_{nf}\frac{\partial T}{\partial r}\Big|_{r=a} = -k_{nf}\frac{\Delta Tr}{a}\sqrt{\frac{U_w}{\nu_f z}}\theta'(\eta)\Big|_{r=a} \qquad (22)$$

$$m_w = -Dm\frac{\partial C}{\partial r}\Big|_{r=a}$$

Using the dimensionless variables we obtain

$$Re_z^{\frac{1}{2}} C_{fz} = \frac{\phi_1}{\phi_2}[f''(0) + Wef''^2(0)],$$

$$Re_z^{-\frac{1}{2}} N u_z = (-\theta'(0)), \qquad (23)$$

$$Re_z^{-\frac{1}{2}} S\square_z = (-\phi'(0))$$

Local Reynold's number $Re_z = \frac{U_w z}{\upsilon_{nf}}$

## III. METHOD OF SOLUTION

The Homotopy Perturbation Method (HPM) is employed in this work to obtain the exact analytical solution. This approach is required due to the complex structure of the reduced set of similarity equations. The equations are coupled and nonlinear, which makes it difficult to find exact solutions.It is crucial to select Homotopy Perturbation Method (HPM) because it effectively combines homotopy theory with perturbation theory. The primary concept is to transform a complex issue into a simpler one through continuous deformation, making it easier to find an exact or approximate analytic solution.

**3.1.2 Analysis of the Nonlinear Model**

In the same way, the governing equation of the model can be converted to dimensionless forms by employing the similarity transformation defined in (11 and 12)

Consider the following system of nonlinear ordinary differential equations: there are six equations in total**.** The equations governing the fluid and dust phases are those that describe the velocity energy and concentration equations respectively.

**Equation of velocityfor the fluid phase model**

$$\phi_1\{(1+2\gamma\eta)f'''(\eta)+2\gamma f''\}+\phi_1\lambda(1+2\gamma\eta)^{\frac{1}{2}}[\gamma f''^2+2\{\gamma f''+(1+2\gamma\eta)f'''\}]+\phi_2(f(\eta)f''(\eta)-f'^2)-l\beta_v\left(f'(\eta)-F'(\eta)\right)-(M+K)f'(\eta)=0 \quad (24)$$

**Equation ofEnergy for the fluid phaseConcentration equation for the fluid phase**

$$\frac{\phi_1\phi_4}{Pr}\{(1+2\gamma\eta)\theta''+2\gamma\theta'\}+\phi_1\phi_3(\theta' f-2\theta f')+N_b\phi'\theta'+N_t\theta'^2+\phi_1\phi_2\, l\beta_t\left(\theta_p-\theta\right)+M.l\beta_t Ec\left(F'(\eta)-f(\eta)\right)=0 \quad (25)$$

$$\phi''+Lef\boldsymbol{\phi}'+\left(\frac{\mathbf{N_T}}{\mathbf{N_B}}\right)\theta''=0 \quad (26)$$

**Velocity equation for the dust phase model**

$$F'^2-FF''-\beta_v(f'-F')=0 \quad (27)$$

**Energy equation for the dust phase**

$$\theta_p'F-2\theta_pF'+\gamma^*\beta_T\left(\theta-\theta_p\right)=0 \quad (28)$$

**Concentration equation for the dust phase**

$$\phi_p'F-2\phi_pF'+l\beta_cH\left(\phi_p-\phi\right)=0 \quad (29)$$

## IV. Results and Discussion

4.1**Verification of results**

This section presents the simulations of the implemented numerical solutions. Table 1 displays the several values of M for the temperature profile θ'(0) and was compared to the results of Kumar et al. [18]Manjunatha et. al. [19]. The results of the present study are in excellent agreement. In the same vein, Table 2 displays a variety of M values for the velocity profile f"(0). These values were compared to the findings of Chen [8], Giresha [10], and Ramesh et al [26] and were found to be in excellent accord with the existing published results. The Nusselt number and Sherwood number are augmented by different magnitudes of the observed parameters The table illustrates that the local Nusselt number increases as the Prandtl number increases, while the Sherwood number decreases. This serves as confirmation that the HPM employed in this investigation is precise and flawless. This demonstrates the validity of the current results and the precision of the current analytical technique. We are therefore confident in the high accuracy of our findings in the analysis of this boundary layer flow problem.

| $Ha$ | Kumar*et al*. [16] $f''(0)$ | Present work (HPM) $f''(0)$ | Giresha *et al.* [22] $-\theta'(0)$ | Present work (HPM) $-\theta'(0)$ |
|---|---|---|---|---|
| 0.72 | $-0.3645$ | 0.3645 | $-1.08850$ | $-1.08850$ |
| 1.0 | $-1.41425$ | $-1.41425$ | $-1.3333$ | $-1.3333$ |
| 3.0 | $-160873$ | $-160873$ | $-1.4287$ | $-1.4287$ |
| 5.0 | $-2.44948$ | $-2.44948$ | $-1.5295$ | $-1.5295$ |
| 10 | $-3.31662$ | $-3.31662$ | $-2.2960$ | $-2.2960$ |

Table 1 Comparison of the present results for the dimensionless temperature gradient-θ'(0) and $\boldsymbol{f''(0)}$with previous published work of Kumar et al and Gıresha et. al. respectively

| $\nu$ | $\sigma$ | $Ha$ | $K$ | $C_f$ | Nu | Sh |
|---|---|---|---|---|---|---|
| 2 | | 0.5 | | -3.7 757 | 4.269967 | 13.9999 |
| 4 | 2 | | -2 | -3.70327 | 4.249719 | 13.4527 |
| 6 | | | | -3.67615 | 4.241769 | 13.2368 |
| 6 | 2 | 0.5 | | -3.70327 | 4.249719 | 13.4527 |
| | 4 | | -2 | -3.69998 | 4.243165 | 13.4073 |
| | 6 | | | -3.69869 | 4.243022 | 13.3902 |
| 6 | 2 | 1 | | -3.86581 | 4.243082 | 13.4460 |
| | | 2 | -2 | -4.16282 | 4.2431584 | 13.4344 |
| | | 3 | | -4.43051 | 4.221891 | 13.4247 |
| 6 | 2 | 0.5 | -3 | -4.57301 | 5.056291 | 15.46842 |
| | | | -2 | -3.70327 | 4.249719 | 13.45271 |
| | | | -1 | -2.93163 | 3.607416 | 11.52169 |

Table 2:Effects of $\upsilon, \sigma, M, and S$ on Skin Friction coefficient $C_f$ , Nusselt number (Nu) and Sherwood number (Sh)

**The Effects of Physical Parameters on the dimensionless Velocity Profile**

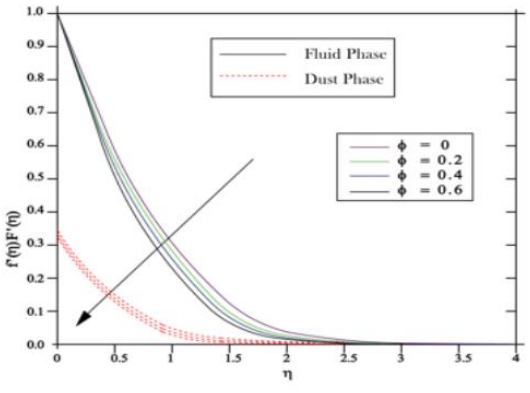


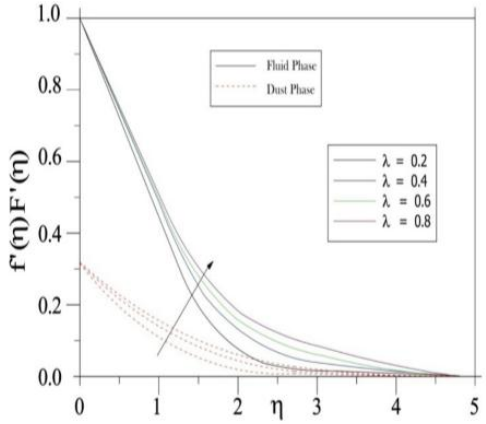


Figure: 2 Effect of volume fraction parameter on on the velocity of fluid and dust phases

Figure3: Effect of Wesseinberg Parameter on the velocity profile of fluid and dust phase

Figure 2, shows the effect of volume fraction parameter on fluid and dust phases. It is clear that an increase in the volume fraction of dust particles leads to decrease in the velocity profile for both the fluid and dust phases, this is because the volume occupied by the dust particles per unit volume of mixture is high than the dust concentration and also the nanofluid viscosity will increase as there exist a direct relationship or proportion between the two parameters. As a result, the increasing viscosity resists the fluid motion along the stretching direction leading to the slowdown of the fluid flow. This causes a decrease in the momentum boundary layer thickness and increase in the mass concentration of the dust phase. An increment in dust particle volume fraction improve the drag force within the fluid and therefore, velocities are reduced. Figure 3 depict the effects of Weissenberg parameter (We) , $\lambda$, on the fluid and dust phases velocity distribution. Increasing the $\lambda$ parameter reduces the magnitude of the fluid velocity for shear thinning fluid while it arises for the shear thickening fluid. The ratio of relaxation time to retardation time is represented by the Wesseinberg parameter, $\lambda$. As the values of $\lambda$, rise, the relaxation time of fluid molecules similarly increases. This leads to an augumentation in dynamic viscosity, which in turn causes obstructions to the movement of the fluid, thus leading to a reduction in fluid flow. Furthermore, it has been shown that the velocity of dust particles increases while that of the fluid decreases. The conclusion can be deduced from the observation that an augmentation in the $\lambda$ , has an adverse impact on the dust particle velocity relaxation time causing the particles to adjust to become parallel with the fluid velocity.

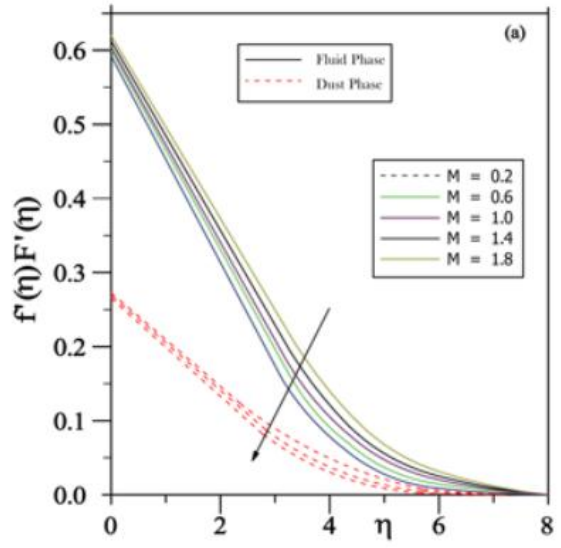


**Figure 4: Effect of Magnetic parameter on velocity profile of fluid and dust phases**

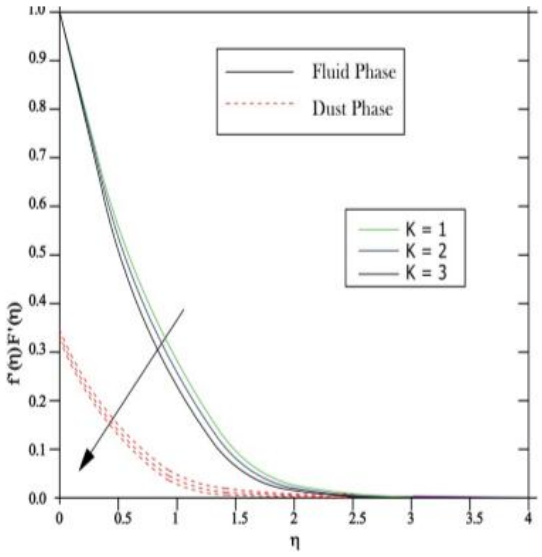


**Figure 5: Effect of Porosity parameter on velocity profile of fluid and dust phases**

Figure 4 shows the effect of the strength of the magnetic field parameter, M, on the fluid phase and dust phase velocity distribution. It is noticeable that the result of this effect is negative in the sense that the relationship between the magnetic field and the velocity distribution is inverse. The increase in the values of the magnetic field means a decrease in the velocity of the fluid. Physically, when a moving fluid is influenced by the magnetic field, the fluid particles are stimulated, which creates a kind of counter force that slows and reduces the fluid's motion. Moreover, this resistive drag force known as the Lorentz force is perpendicular to the velocity vector on the one hand and also perpendicular to the magnetic field vector on the other hand, while highlighting that the increase in the magnetic field reduces the thickness of the boundary layer. Fig 5 depicts the influence of porosity parameter on the fluid and dust phases velocity profile. An augmentation in the porosity parameter results in a decrease in the permeability of the porous material, leading to a decrease in the velocity profile for both fluid and dust phases. As a result, the thickness of the boundary layer reduces. An augmentation in the porosity parameter results in a reduction in the surface drag force. The presence of larger pore size in the medium creates a resistance to fluid movement. Furthermore, the existence of the porous material reduces the movement of the fluid as a result of the velocity interaction parameter. The velocity gradient of the fluid and dust phases decreases steadily as the porosity parameter value increases.

### 4.3 The Effects of Physical Parameters on the Dimensionless Temperature Profile.

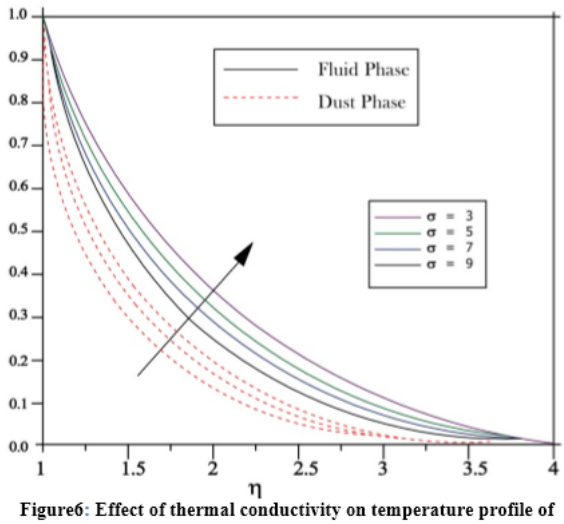


**Figure6: Effect of thermal conductivity on temperature profile of fluid and dust phases.**

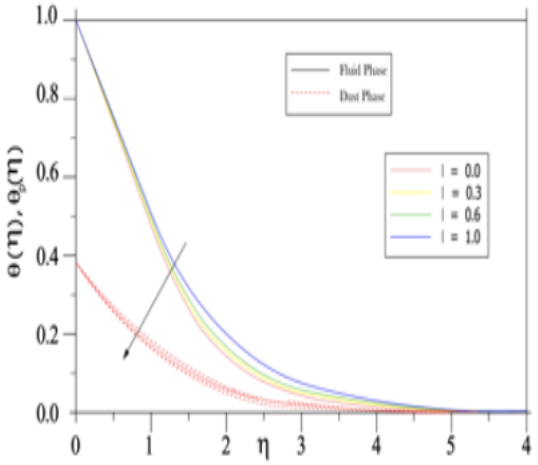


**Figure 7: Effect of mass concentration on temperature profile of fluid and dust phases.**

Figure 6 illustrates the impact of variation of thermal conductivity on the fluid and dust phases' temperature profile. An augmentation in the thermal conductivity parameter results in an increase of the temperature of both the fluid and dust phases. Hence thermal conductivity variation must not be disregarded. Furthermore augmentation of the value of temperature is quite important signifying that as σ increases, the flow rate in the corresponding crosssection of the cylinder increases. The effect of mass concentration l, on the temperature profiles for both fluid and dust phases are displayed in Figure 13. It is clear from the figures that an increase in l causes a decline in the temperature profiles of fluid and particle phases. It is obvious that increase in mass concentration of dust particles reduces the temperature boundary layers. When the dust particles are suspended in the clean fluid, they cause resistance within the fluid at regular intervals. Furthermore, the dust particles absorb heat from the fluid upon contact. Consequently, the thermal boundary layer thickness decreases.

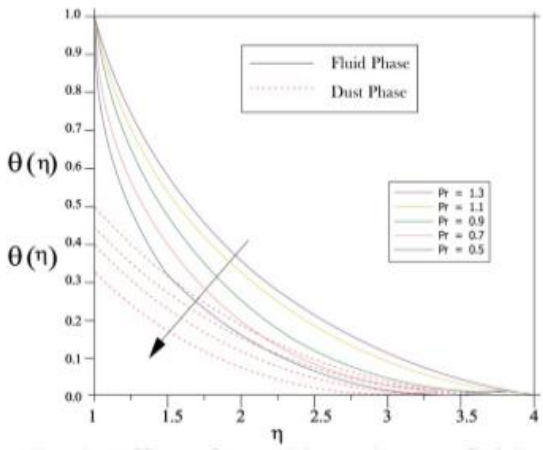


Figure 8: Effect of Prandtl number on temperature profile of fluid and dust phases.

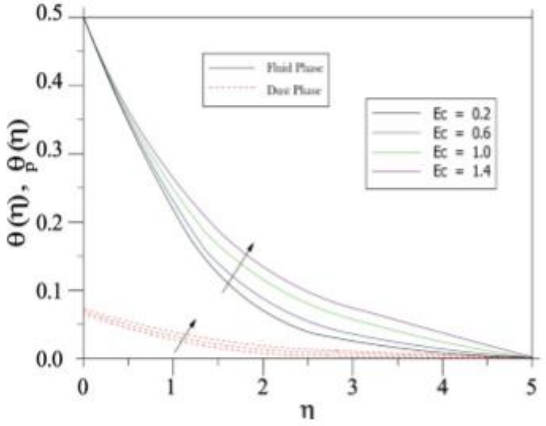


Figure 9: Effect of Eckert number on temperature profile of fluid and dust phases.

The change in the fluid temperature plays an important role in the fluid's behavior in addition to its effect also on the particles inside the fluid. Fig-8 shows the variation of non dimensional temperature pro-file for various values of Prandtl number, Pr. The Prandtl number can be viewed as the ratio of momentum to thermal boundary layers. Physically, a high Prandtl number means a small thermal boundary layer this increases the gradient of the temperature. It is observed that an increase in the value of Pr leads to a decrease of temperature pro-files in the fluid phase. The physical reason is that the lower values of Pr mean a lower viscosity of the fluid, which increases the local velocity everywhere within the boundary layer. Thus, the higher Prandtl number fluid has a relatively low thermal conductivity which reduces the conduction. In heat transfer problems, the Prandtl number controls the thickness of the momentum and thermal boundary layer. Fluids with lower Prandtl number

have higher thermal conductivities so that heat can diffuse from the cylinder faster for higher Prandtl number. Figure 9 represents the effect of Eckert number on the temperature distribution of the fluid and dust phases. The plot shows that increasing the Eckert number also increases the temperature profile as well as the thickness of the boundary layer. Higher values of the Eckert number amplify the movement and energy of fluid molecules. This is due to the fact that greater viscous dissipative heat causes a rise in temperature profile and the heat energy is stored in liquid with the frictional heating, that is, the viscosity of fluid takes the energy from motion of the fluid and converts it into internal energy of fluid, re-sulting in a rise in the fluid's temperature whilst the temperature of dust phase decreases with increasing value of Eckert number.

**4.4 The Effects of Physical Parameters on the Dimensionless Concentration Profile.**

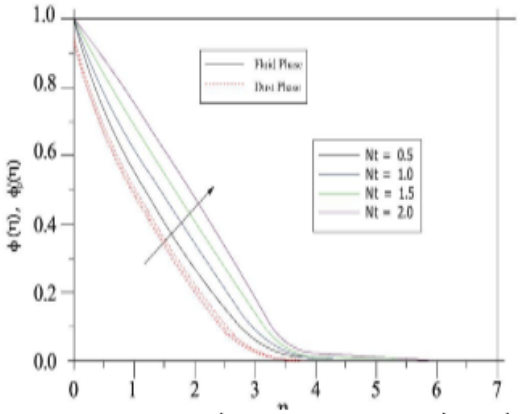


Figure10: Effect of Thermophoresis parameter on concentration profile of fluid and dust phases.

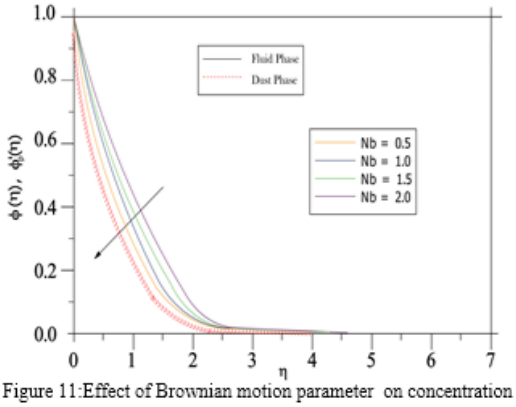


Figure 11:Effect of Brownian motion parameter on concentration profile of fluid and dust phases.

The study of the concentration of nanoparticles within a fluid plays an important role in the properties and applications of this fluid from several sides; for example, the degree and efficiency of the thermal conductivity of a nanofluid are related to the concentration of nanoparticles inside it, and also, the degree and efficiency of its electrical conductivity are related to the concentration of nanoparticles.Figure 10 shows the effect of thermophoresis parameter ($Nt$) on the concentration profile of the fluid and dust phases. A higher value of Nt improves the profile of fluid concentration. The phenomenon known as thermophoresis, occurs when nanoparticles move from an area of higher temperature to a region of lower temperature. This demonstrates how Nt aids in nanoparticle diffusion in the boundary layer, and as a result, there is an indirect correlation observed between the concentrations of $\phi$ *and* $\phi_p$ and Nt. It is discovered that thermophoresis elevates the concentration field, as seen in figure 10. Figure 11 depicts the impact of Nb on the concentration profile . An increase in the value of Nb results in a decrease in fluid concentra-tion and dust phase. The phenomenon of Brownian motion, Nb, de-scribes the irregular trend movement found in the nanoparticles by its suspension in the base fluid. The thermal energy is generated by the dispersion and random motion of nanoparticles. Particles that are evenly distributed have a lower fluid concentration and dust phases Also, the concentration boundary layer thickness becomes very low because of an increase in the Brownian motion parameter (Nb).

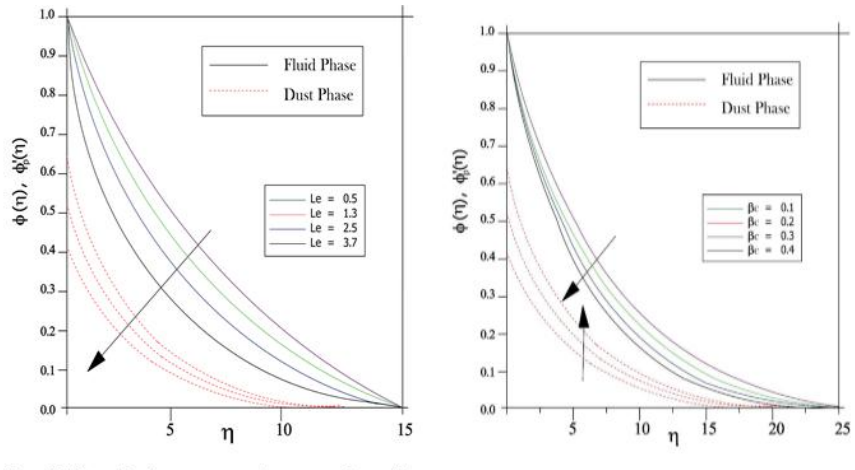


Figure 12:Effect of Lewis parameter on the concentration profile

Figure 12,shows the influence of Lewis parameter on fluid and dust phases. The Lewis number is applicable in scenarios where concurrent heat transfer and mass transfer take place, such as in combustion processes, chemical reactions, and heat exchangers. The Lewis number quantifies the ratio of rate of heat transfer to that of mass transfer rate in a fluid. A low Lewis number signifies that thermal energy diffuses at a faster rate than mass, whereas a high Lewis number implies that mass diffuses at a faster rate than thermal energy. Understanding the Lewis number is crucial for forecasting temperature profiles and concentration distributions in systems where both heat and mass transfer play a significant role. From fig 12, it is evident that an elevation in the Lewis number, Le, leads to a reduction in the concentration profiles of both the fluid and dust phases. As anticipated, the mass diffusivity rises proportionally to the increase in Le, resulting in a decrease in the thickness of the concentration boundary layer. Fig. 13 clearly demonstrates that raising the fluid-particle interaction parameter for concentration, $\beta_c$, leads to a drop in the fluid phase concentration profiles and an enhancement of the dust phase profiles. This could be attributed to the high interaction between the fluid and dust phases when dust particles is introduce into the flow, resulting in an enhanced concentration profile of the dust phase.

## V. CONCLUSION AND CONTRIBUTIONS TO KNOWLEDGE

### 5.1 Conclusion

- This study examines the flow of a two-dimensional Williamson MHD Nanofluid flow past a stretching permeable cylinder immersed in a porous medium. The mathematical equations of this two-phase flow model are solved by using the Homotopy perturbation Method on Matlab software. The work graphically presents and discusses the impacts of various governing parameters on the velocity and temperature profiles, as well as the skin friction coefficient and Nusselt parameter. The main findings of this investigation are as follows:
- Increasing values of Magnetic parameter result in a reduction in the fluid and dust phase velocity. as well as the momentum boundary layer thickness.
- Increase in porosity parameter result in a drag force that reduces the velocity of the fluid. Hence the velocity gradient of the fluid and dust phases increase steadily with increase in porosity parameter
- .Increasing the volume fraction of the dust particles result in reduction of the velocity profiles and enhances the temperature profiles of both phases.
- Wesseinberg parameter decreases the rate of flow and the boundary layer thickness in the fluid phase but increases the rate of flow and boundary layer thickness in the dust phase
- Increase in the value of Prandtl number, Pr leads to a decrease of temperature profiles in the fluid phase. Thus, higher Prandtl number fluid has a relatively low thermal conductivity which reduces the conduction.
- High values of Lewis number leads to a reduction in the concentration profiles of both the fluid phase and dust phase. Understanding the Lewis number is crucial for forecasting temperature profiles and concentration distributions in systems where both heat and mass transfer play a significant role
- Magnetic number has the tendency to reduce the skin friction coefficient and Nusselt number. Also an increase in magnetic field parameter and porosity parameters contribute to a gradual decrease in the skin friction coefficient.

### 5.2 Contributions to Knowledge

The following contributions are made in advancement of the body of knowledge:

i. The uniqueness of this current study is the addition of dusty particles to Williamson nanofluid. Also researchers realized the difficulty of nonlinear coupled differential equations and have not been able to solve the problem using analytical method, but always with numerical methods . Therefore this research work has succeeded in using analytical method (HPM) to solve the modeled problems

ii. This work developed hydrothermal flow model considering dust and nanoparticle in the flow.

iii. This work provided analytical solutions for the coupled Nanofluid dust hydrothermal flow model behaviour.

**ACKNOWLEDGEMENTS**

The authors are grateful to the authors referred in this work.

**CONFLICTS OF INTEREST**

The authors declare no conflict of interest

## REFERENCE


[1]. Williamson, R.V. The flow of pseudoplastic materials, Industrial and Engineering Chemistry,(1929) : vol. 21, no. 11, pp. 1108–1111.

[2]. Subbarayudu, K. Suneetha, S. and Reddy, P. B. A. The assessment of time dependent flow of Williamson fluid with radiative blood flow against a wedge, Propulsion and Power Research, (2020): vol. 9, no. 1, pp. 87–99.

[3]. Hashim, A. Hamid, M. Khan, Multiple solutions for MHD transient flow of Williamson nanofluids with convective heat transport, (2019): Journal of the Taiwan Institute of Chemical Engineers,Vol. 103, pp. 126-137,

[4]. Jiang, P., Ren, Ze-Pei, Numerical investigation of forced convection heat transfer in porous media using a thermal non-equilibrium model, 200: International Journal of Heat and Fluid Flow

[5]. Masuda, H.; Ebata, A.; Teramae, K.; Hishinuma, N. Masuda, H.; Ebata, A.; Teramae, K.; Hishinuma, N. Alteration of Thermal Conductivity and Viscosity of Liquid by Dispersing Ultra-Fine Particles. Dispersion of Al2O3, SiO2 and TiO2 Ultra-Fine Particles. NetsuBussei 7, 227–233. Alteration of Thermal Conductivity and Viscosity of Liquid by Dispersing Ultra-Fine Particles. Dispersion of Al2O3, SiO2 and TiO2 Ultra-Fine Particles. (1993): NetsuBussei: 7, 227–233.

[6]. Choi, S.U. and Eastman, J.A. Enhancing Thermal Conductivity of Fluids with Nanoparticles, (1995): Argonne National Lab.(ANL), Argonne, IL, USA, vol. 231, pp. 99–106

[7]. Elboughdiri, N.; Ghernaout, D.; Muhammad, T.; Alshehri, A.; Sadat, R.; Ali, M.R.; Wakif, A. Towards a novel EMHD dissipative stagnation point flow model for radiating copper-based ethylene glycol nanofluids: An unsteady two-dimensional homogeneous second-grade flow,(2023): Case Study. Therm. Eng., 45, 102914

[8]. Alfvén, H. Existence of Electromagnetic-Hydrodynamic Waves. 1942: Nature 150, no. 3805, pp.405–406.

[9]. Amjad, M. Ahmed, I. Ahmed, K. Alqarni, M.S. Akbar, T. Muhammad, T. Numerical Solution of Magnetized Williamson Nanofluid Flow over an Exponentially Stretching Permeable Surface with temperature dependent viscosity and thermal conductivity, (2022): Nanomaterials, vol.12, pp. 3661.

[10]. Reddy S.C, Kishan, N. and Mohammad M.R.: MHD flow and heat transfer characteristics of Williamson nanofluid over a stretching sheet with variable thickness and variable thermal conductivity, (2017): Transactions of A. Razmadze Mathematical Institute, Vol. 171, Issue 2, Pages 195-211.

[11]. Abbas, N., Nadeem, S., Saleem, A., Malik, M.Y., Issakhov, A. and Alharbi, F.M. Models base study of inclined MHD of hybrid nanofluid flow over nonlinear stretching cylinder. (2021): Chin. J. Phys., vol.69, pp.109–117.

[12]. Mahdi, R.A., Mohammed, H.A., Munisamy, K.M., Saeid, N.H. Review of convection heat transfer and fluid flow in porous media with nanofluid. Renew. Sustain. Energy Rev. (2015), 41, 715–734.

[13]. Kothandapani, M. and Srinivas, S. (2008): On the influence of wall properties in the MHD peristaltic transport with heat transfer and porous medium. Phys. Lett. A 372, pp.4586–4591.

[14]. Adekanmbi-Akinseye O.A., Fenuga O.J., Isede H.A., Sobamowo M.G. (2024): Flow and heat transfer of a dusty Willimason MHD Nanofluid flow over permeable cylinder in a porous medium, OJFD: Vol 14 No 2.


## NOMENCLATURE

$u$, w Fluid-phase velocity components

$u_p$ , $w_p$ Dust-phase velocity components

$\mu$ Dynamic viscosity

$\nu$ Kinematic viscosity

$q_w$ Thermal flux at the fluid temperature surface

$T_w$ Wall temperature

$T_P$ Temperature of the dust particle

T Temperature of the Nano fluid

$T_\infty$ Ambient Temperature

$D_m$ Mass diffusivity

I Identity tensors

M Magnetic fluid parameter

$q_w$ Thermal flux

λ Wesseinnberg number

$V_w$ Velocity at the wall

β Fluid particle interaction parameter

$\theta$: Dimensionless temperature

$\theta_p$ Dimensionless temperature for the dust particle

S: Heat source/sink parameter

$B_0$ Magnetic field strength

$C_{fz}$ Skin-friction coefficient

$Nu_z$ local Nusselt number

$Re_z$ Reynolds number

$f, f'$ Dimensionless velocities of fluid phase

$F, F'$ Dimensionless velocities of dust phase

$K_p$ Permeability of the dust particle

$D_B$ Brownian diffusion coefficient [m2 s−1]

$D_T$ Thermophoresis diffusion coefficient [m2 s−1]

$\tau_V$ The relaxation time of dust particles

M Magnetic parameter

Pr Prandtl number

Nf Nanofluid

Ec Eckert number

Ha Hartman's number

$\sigma$ Electrical conductivity

$\alpha$ Thermal diffusivity

Γ Positive time constant

$K$ Porosity parameter

$f_w$ Volumetric fraction parameter

ψ Stream function

$\gamma$ Curvature parameter